AGU ADVANCING EARTH AND SPACE SCIENCE

Geophysical Research Letters

RESEARCH LETTER

10.1029/2022GL099925

Recent Increase in the Occurrence of Snow Droughts Followed by Extreme Heatwaves in a Warmer World

Xiangfei Li[1] and **Shuo Wang**[1,2]

[1]Department of Land Surveying and Geo-Informatics and Research Institute for Land and Space, The Hong Kong Polytechnic University, Hong Kong, China, [2]Shenzhen Research Institute, The Hong Kong Polytechnic University, Shenzhen, China

Key Points:

- There is a significant spatial expansion (13%) of compound snow drought and heatwave (CSDHW) events in the snow-covered area of Eurasia
- The warm-type CSDHW becomes more frequent and expands faster than the dry-type CSDHW
- Dry snow drought promotes the occurrence of subsequent heatwave associated with intensified soil drought and atmospheric aridity

Supporting Information:

Supporting Information may be found in the online version of this article.

Correspondence to:

S. Wang,
shuo.s.wang@polyu.edu.hk

Citation:

Li, X., & Wang, S. (2022). Recent increase in the occurrence of snow droughts followed by extreme heatwaves in a warmer world. *Geophysical Research Letters*, *49*, e2022GL099925. https://doi.org/10.1029/2022GL099925

Received 6 JUN 2022
Accepted 18 JUN 2022

Author Contributions:

Conceptualization: Shuo Wang
Data curation: Xiangfei Li
Formal analysis: Xiangfei Li
Funding acquisition: Shuo Wang
Investigation: Shuo Wang
Methodology: Xiangfei Li
Project Administration: Shuo Wang
Resources: Shuo Wang
Software: Xiangfei Li
Supervision: Shuo Wang
Validation: Xiangfei Li
Visualization: Xiangfei Li
Writing – original draft: Xiangfei Li
Writing – review & editing: Shuo Wang

Abstract The compound of late winter snow droughts and early spring heatwaves (compound snow drought and heatwave (CSDHW)) could dramatically affect ecosystems and water availability, but has not been systematically investigated. Here we present a comprehensive assessment of CSDHW events and possible driving mechanisms. We find that 7% of the snow-covered area experiences significant ($p < 0.05$) CSDHW events, and an average of 35% of snow droughts are followed by heatwaves during 1981–2020. The spatial extent of CSDHW is asymmetrically enlarging, with a significant increase in Eurasia and a relatively high fluctuation in North America. Specifically, the warm-type CSDHW (i.e., snow drought with normal or above-average precipitation followed by heatwave) occurs more frequently, with spatial coverage increasing faster than the dry-type CSDHW (i.e., snow drought with below-average precipitation followed by heatwave). In comparison, dry snow drought is more likely to be followed by heatwave due to intensified soil drought and atmospheric aridity.

Plain Language Summary Snow drought and heatwave events have adverse impacts on society and ecosystems, and have drawn much attention in the past decades. However, the consecutive occurrence of the two extreme events remains poorly understood. This study presents a global assessment of compound snow drought and heatwave (CSDHW) events for the period from 1981 to 2020. We find that more than one third (35%) of snow droughts are followed by heatwaves. The spatial extent of CSDHW is expanding globally, with a significant increase in Eurasia and a relatively high fluctuation in North America. Despite the higher frequency and expanding trend of the warm-type CSDHW (i.e., snow drought with normal or above-average precipitation followed by heatwave) than the dry-type CSDHW (i.e., snow drought with below-average precipitation followed by heatwave), dry snow drought is more likely to be followed by heatwaves, which can be attributed to intensifying soil drought and atmospheric aridity after dry snow drought.

1. Introduction

Snow drought is a period of unusually low snowpack for the time of year (Harpold et al., 2017). Heatwave occurs in a period of prolonged abnormally high surface temperatures relative to those normally expected (Robinson, 2001). Previous studies have investigated snow droughts and heatwaves individually (Chen & Zhai, 2017; Dierauer et al., 2019; Huning & AghaKouchak, 2020; Perkins-Kirkpatrick & Lewis, 2020). Nevertheless, little effort has been made to investigate the consecutive occurrence of snow drought and heatwave, namely compound snow drought and heatwave (CSDHW).

There is a close connection between snow drought and heatwave. For instance, snow is featured with high albedo and high latent heat that could influence the energy partition processes on the land surface and thus the climate system (Déry & Brown, 2007; Matsumura & Yamazaki, 2012). Snow is also known as a natural water reservoir, which is a crucial recharge source of soil moisture (SM) in spring (Barnett et al., 2005; Qi et al., 2020). The characteristics of snow cover are closely related to heatwave, which is associated with high temperature and regulated by local-scale conditions (e.g., SM conditions) in the lower atmosphere (Jaeger & Seneviratne, 2011; Stegehuis et al., 2021). In the context of declining snow cover (Déry & Brown, 2007), it is possible that heatwave is associated with preceding snow drought, potentially leading to an emerging compound hazard. Moreover, growing evidence shows that the vanishing snow contributes to the occurrence of heatwave. Many studies have demonstrated that the heatwaves across northern mid-latitudes are closely linked to the reduction in snow cover (Francis & Vavrus, 2012; Tang et al., 2014; Zhang et al., 2020). A recent example is the unseasonable heatwave in California in February 2022, which occurred after a prolonged period without measurable precipitation during winter (The Guardian, 2022).

Given that snow drought and heatwave can damage ecological (Christensen et al., 2013; Trujillo et al., 2012), agricultural (Malek et al., 2020), and social systems (Kovats & Hajat, 2008; Wlostowski et al., 2022), the sequential occurrence of the two extreme events is expected to amplify the risk for natural and human systems (Raymond et al., 2020). For example, the western U.S. has been witnessing a reduction in snowfall and an increase in cascading disasters in recent years (Marshall et al., 2019; Mote et al., 2018; Nexus Media, 2018). The dwindling snowpack has not only put California's water supply at risk but also has triggered increasing wildfires due to the resulting dry conditions and hot weather (Gleason et al., 2019). In addition, the loose soil after wildfires, combined with intense rainfall, may initiate mudslides during a rainy season (Oakley et al., 2017). Another example is the 2010 droughts in the southern Volga District of Russia and northern Kazakhstan, where precipitation was less than 30% of normal from April to July. The drought contributes to the following heatwaves in Russia in July and August, slashing crop production, sparking thousands of wildfires, and resulting in as many as 15,000 deaths (LeComte, 2011).

Despite the widely recognized connections between snow reduction and heatwave as well as their severe impacts, few studies have focused on the consecutive snow drought and heatwave events (i.e., CSDHW). A holistic picture of global hotspots and evolutionary processes of CSDHW events is lacking. Furthermore, little is known about potential interrelationships between snow drought and heatwave characteristics. Physical mechanisms causing the occurrence of CSDHW events also remain unclear.

To address the above-mentioned issues, we perform an in-depth analysis of spatiotemporal variation in CSDHW events and possible mechanisms that trigger heatwaves after snow droughts over the snow-covered area. This study will shed light on the understanding of emerging CSDHW hazards and their dynamic evolution over a 40 year period from 1981 to 2020.

2. Data and Methods

2.1. Data

The enhanced global data set for the land component of the fifth generation of European ReAnalysis (ERA5-Land) was used in this study. We used monthly snow water equivalent (SWE) and precipitation (P) to calculate the nonparametric standardized index for SWE (SWEI) and precipitation (SPI), and then to identify snow drought events. Daily maximum 2 m temperature (T_{max}), aggregated from the 1 hourly T_{max}, was adopted to identify heatwaves. Monthly SM and vapor pressure deficit (VPD) were also used to investigate the connections between snow drought and heatwave. VPD was calculated from monthly air temperature and dewpoint temperature (Yuan et al., 2019). All datasets covered a 40 year period from 1981 to 2020 and were gridded to 0.25° spatial resolution using the bilinear interpolation method. Additionally, the Moderate Resolution Imaging Spectroradiometer/Terra (MODIS/Terra) Monthly Snow Cover data set (MOD10C1) spanning from March 2003 to September 2021 (Hall & Riggs, 2015), together with the monthly SWE from ERA5-Land, were used to mask the snow-covered area and the first snow-free month. Reference regions of the Fifth Assessment Report of the United Nations Intergovernmental Panel on Climate Change AR5 (IPCC AR5) were used to look into details in sub-regions (Christensen et al., 2013).

2.2. Identification of Snow-Covered Area and Extreme Events

The processes of determining the global snow-covered area followed the study of Huning and AghaKouchak (2020). We calculated the 3 month average snow cover (SC) climatologies using the MODIS/Terra data and then applied a 5% SC threshold to extract the initial snow-covered area. Then the snow-covered area was further refined with the ERA5-Land data by considering the land grid boxes where at least 75% of a given month for all years was covered by snow (with non-zero SWE value). The snow-covered area can be seen in Figure S6 of Supporting Information S1.

In this study, the CSDHW event refers to the snow drought in the last snow-covered month followed by heatwaves occurring in the first snow-free month during a year. The first snow-free month is defined as the month when SC climatology is below 5% for the first time based on the MODIS/Terra snow cover data, before which is the last snow-covered month (Huning & AghaKouchak, 2020; Smith et al., 2017; Toure et al., 2018). As illustrated in Figure S6 of Supporting Information S1, grid boxes do not necessarily have the same first snow-free month.

Snow drought is identified based on the SWEI at the 3 month scale, which is analogous to the calculation of 3 month SPI (Huning & AghaKouchak, 2020). When the SWEI of the last snow-covered month is less than or equal to −0.5, it is identified as a snow drought (Table S1 in Supporting Information S1). Based on previous studies (Dierauer et al., 2019; Harpold et al., 2017; Mote et al., 2016), we further classified snow drought as dry and warm. Dry snow drought is featured with below-normal precipitation, which is identified when the SPI is less than or equal to −0.5 in this study. Warm snow drought has above- or near-normal precipitation and usually results from warm temperatures that cause precipitation falling as rain or unusual snowmelt or both. In this study, warm snow drought is identified if the SPI is greater than −0.5. We emphasize that the precipitation deficit is not the only factor that induces dry snow drought based on our classification. Less precipitation is generally accompanied with higher temperature which may also contribute to the occurrence of dry snow drought (Dierauer et al., 2019). Our classification method of snow drought reflects the meteorological characteristics of snow droughts. Accordingly, the CSDHW with a dry or warm snow drought is termed the dry-type CSDHW or warm-type CSDHW.

For each grid cell, heatwave is identified based on the anomaly in daily T_{max} using the calendar-day 90th percentile (T_{90}). T_{90} is determined using a 15 day moving window for the period of 1981–2020. When the anomaly is positive for at least three consecutive days, it is identified as a heatwave. Note that heatwaves that only occur during the first snow-free month are considered.

Event coincidence analysis is widely used to quantify simultaneous or lagged coincidences of two series of extreme events (Donges et al., 2016; He & Sheffield, 2020; You & Wang, 2021). In this study, we calculated the probability of CSDHW events (i.e., the fraction of snow droughts followed by heatwaves) and examined the significance based on the null hypothesis that CSDHW is randomly distributed as a result of Poisson processes (Donges et al., 2016; Siegmund et al., 2017). The significance test can be seen in Figure S7 of Supporting Information S1.

3. Results

3.1. Hotspots of CSDHW

Figure 1a shows the spatial distribution of the probability of occurrence of CSDHW events, which represents the fraction of snow droughts followed by heatwaves from 1981 to 2020. Approximately 7% of the snow-covered area has experienced statistically significant ($p < 0.05$) CSDHW events and 16% of the snow-covered area has a coincidence rate greater than 50%. On average, 35% of all snow droughts detected in the last snow-covered month are followed by a heatwave event occurring in the first snow-free month.

The CSDHW events are more likely to occur in the arid and transitional regions (AI > 0.9, see Text S1 in Supporting Information S1), and those regions include the inner East Asia (North China & Mongolia), West Siberian, Central Asia, East Europe, and Western North America. The CSDHW events can also be found in some humid areas, such as eastern Canada (Figure 1b). The high frequency of CSDHW in the arid and transitional regions are consistent with the spatial pattern of snow-atmosphere coupling after snowmelt because of the hydrological effect of snow cover (Xu & Dirmeyer, 2011). This implies that snow drought could be memorized in the SM states and compounded with the subsequent heatwaves through land-atmosphere coupling. In addition, the high frequency of CSDHW can be related to atmospheric circulations (Henderson et al., 2018; Tang et al., 2014). For example, the shrinking Eurasian snowpack contributes to enhancing the blocking events by weakening the poleward temperature gradient, and affecting the jet stream and transient eddy activities at mid latitudes, which favors the heatwaves in Europe (Zhang et al., 2020).

3.2. Spatiotemporal Variation of CSDHW

We divided the snow-covered area into 15 sub-regions to investigate the fractions and trends of spatial coverage of dry- and warm-type CSDHW events from 1981 to 2020 (Figure 2). Globally, the warm-type CSDHW occurs more often than the dry-type CSDHW (56% vs. 44%), particularly in high-latitude regions of the Northern

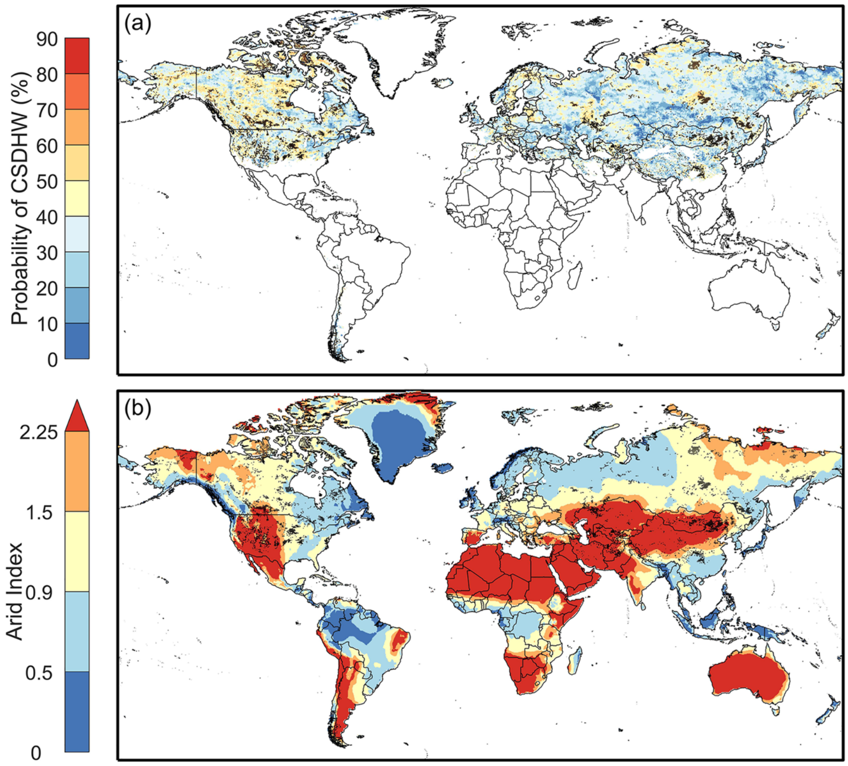

Figure 1. Probability (a) of occurrence of compound snow drought and heatwave (CSDHW) events and Arid Index map (b) showing arid, transitional, and humid regions across the world. Statistically significant grid boxes at 95% confidence level are dotted on maps.

Hemisphere (NEU, CEU, MED, NAS, ENA, ALA and CGI). Southern regions (EAS, TIB, CAS, WAS, ENA, CNA, WNA, SAU, and WSA) generally show comparably fractions of dry- and warm-type CSDHW events.

In terms of the changes in CSDHW events (Figures 2b–2q), the global CSDHW coverage fraction is significantly ($p < 0.05$) increasing at a rate of 2.77%/decade during 1981–2020. All regions across Eurasia (CEU, MED, NAS, EAS, TIB, CAS and WAS) except NEU have a significant ($p < 0.05$) increasing trend in the CSDHW coverage. In particular, NEU, CEU and MED in Europe show a significant increase in the warm-type CSDHW coverage but no trend in the dry-type CSDHW. North America and Southern Hemisphere (CGI, ALA, WNA, CNA, ENA, and WSA) show no significant trends in the CSDHW coverage, except the significant increasing trend of the warm-type CSDHW coverage in SAU. However, the fluctuations of CSDHW coverage in North America are generally higher (e.g., ALA, CNA, and ENA) than those in Eurasia. The warm-type CSDHW generally increase faster than the dry-type CSDHW in most regions, thereby resulting in a global average rate of 1.62%/decade for the warm-type CSDHW in comparison with 1.14%/decade for the dry-type CSDHW.

3.3. Comparison of Heatwave Characteristics Between Dry-Type and Warm-Type CSDHW

We first investigated the heatwave probability (HWP) under different types of snow drought, which represents the fraction of dry or warm snow droughts followed by heatwaves. We find that dry snow drought is more likely to be followed by heatwaves (Figures 3a, 3c, and 3e). And approximately 23% of the snow-covered area experiences a HWP greater than 50% for the period of 1981–2020. For the warm snow drought, however, the proportion falls to 12%. On average, the HWP of dry snow drought is 39% around the globe, about 6% higher than the HWP of warm snow drought (Figure 3e). Moreover, 11 out of the 15 reference regions (NEU, CEU, NAS, EAS, TIB, CAS, WSA, ENA, Central North America, WNA, CGI) have a significantly larger HWP under dry snow drought than warm snow drought. The other 4 regions (MED, SAU, WAS, and ALA) show no significant difference in HWP between the dry and warm snow droughts (Figure 3e). However, dry snow drought has a higher upper quartile than warm snow drought.

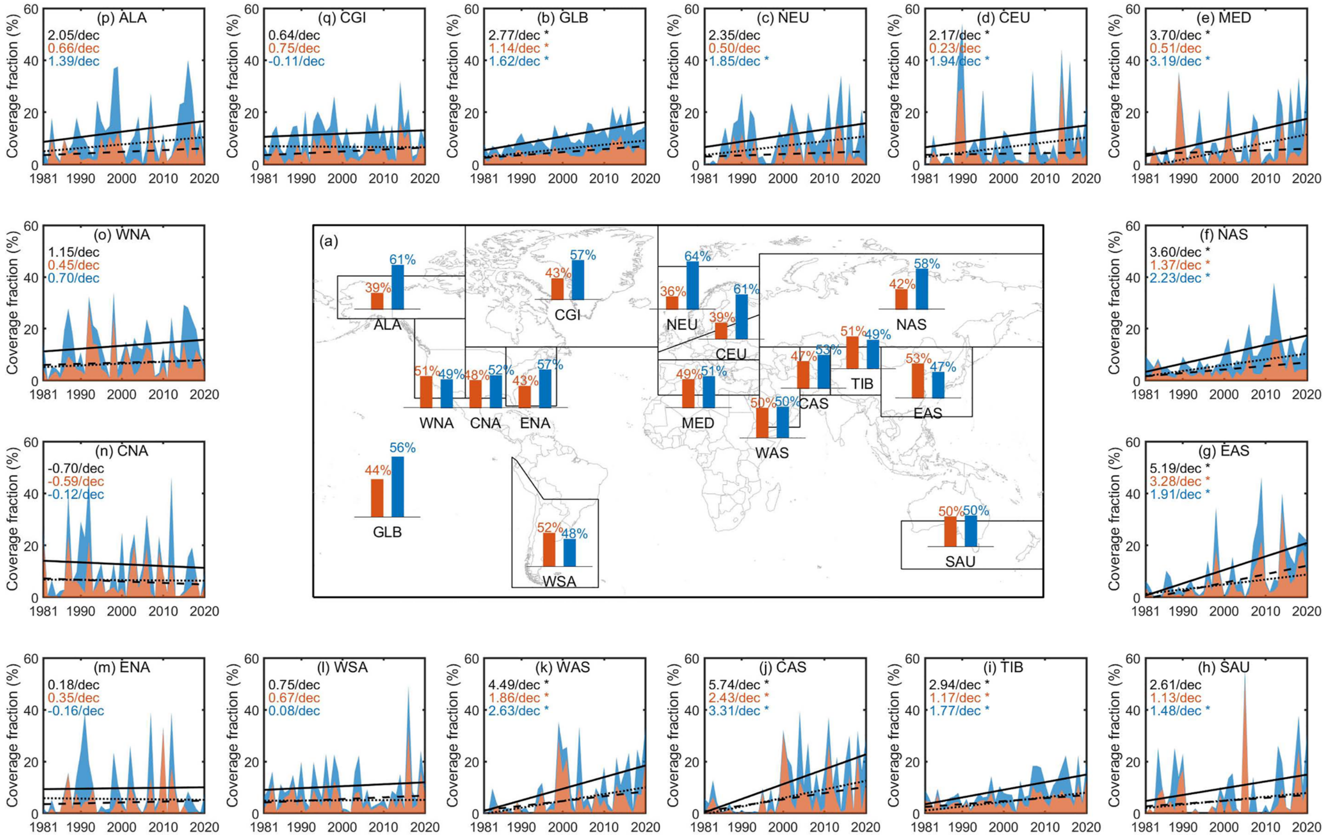

Figure 2. The fractions (a) and spatial coverage trends (b–q) of compound snow drought and heatwave (CSDHW) events across the world during 1981–2020. The red and blue stack areas represent the dry- and warm-type CSDHW events, respectively, the sum of which represents all CSDHW events. The linear annual trends in dry-type, warm-type, and all CSDHW events are represented in dashed, dotted and solid lines, respectively. The number on the left indicates the estimated linear slope based on the least-squares method, and the asterisk denotes the statistically significant trend ($p < 0.05$) based on the Mann-Kendall test. GLB, Globe; NEU, North Europe; CEU, Central Europe; MED, South Europe/Mediterranean; NAS, North Asia; EAS, East Asia; SAU, South Australia/New Zealand; TIB, Tibetan Plateau; CAS, Central Asia; WAS, West Asia; WSA, West Coast South America; ENA, East North America; CNA, Central North America; WNA, West North America; ALA, Alaska/N.W. Canada; CGI, Canada/Greenland/Iceland.

We further examined the heatwave severity (HWS, characterized by the sum of temperature anomaly above T_{90} for all heatwave events) of the dry- and warm-type CSDHW. Dry snow drought tends to be followed by severer heatwave than warm snow drought with highly spatial heterogeneity (Figures 3b, 3d, and 3f). For dry snow drought, approximately 15% of the snow-covered area exhibits the HWS greater than 20°C, which is 3% higher than that of warm snow drought. Globally, the HWS of dry snow drought is 0.9°C higher than that of warm snow drought (Figure 3f). Furthermore, there is a higher HWS of dry snow drought in seven out of 15 reference regions (NEU, CEU, NAS, EAS, CAS, ENA, CGI) compared with the HWS of warm snow drought (Figure 3f), with the most significant differences detected in CEU, NAS, and CGI. Three reference regions (MED, CNA, and ALA) have a higher HWS of warm snow drought than dry snow drought, and the other regions of SAU, TIB, WAS, WSA, and WNA show no statistically significant difference.

3.4. Possible Mechanisms That Trigger Heatwaves After Snow Droughts

To investigate the possible connections between snow drought and the following heatwave, we evaluated the atmospheric and land surface conditions using SM and VPD anomalies (Figure 4). SM can reflect soil drought conditions, and the SM depletion is vital in amplifying temperature through land-atmosphere coupling processes (Dirmeyer et al., 2021; Hirsch et al., 2019; Seneviratne et al., 2010; Stegehuis et al., 2021). VPD measures the atmospheric aridity, and high VPD is often accompanied with high temperature (Horton et al., 2016; Lansu et al., 2020). We first compared the SM and VPD anomalies of the first snow-free month in the snow drought grid boxes with those in all grid boxes (Figures 4a–4d). When dry snow drought occurs, SM (VPD) generally

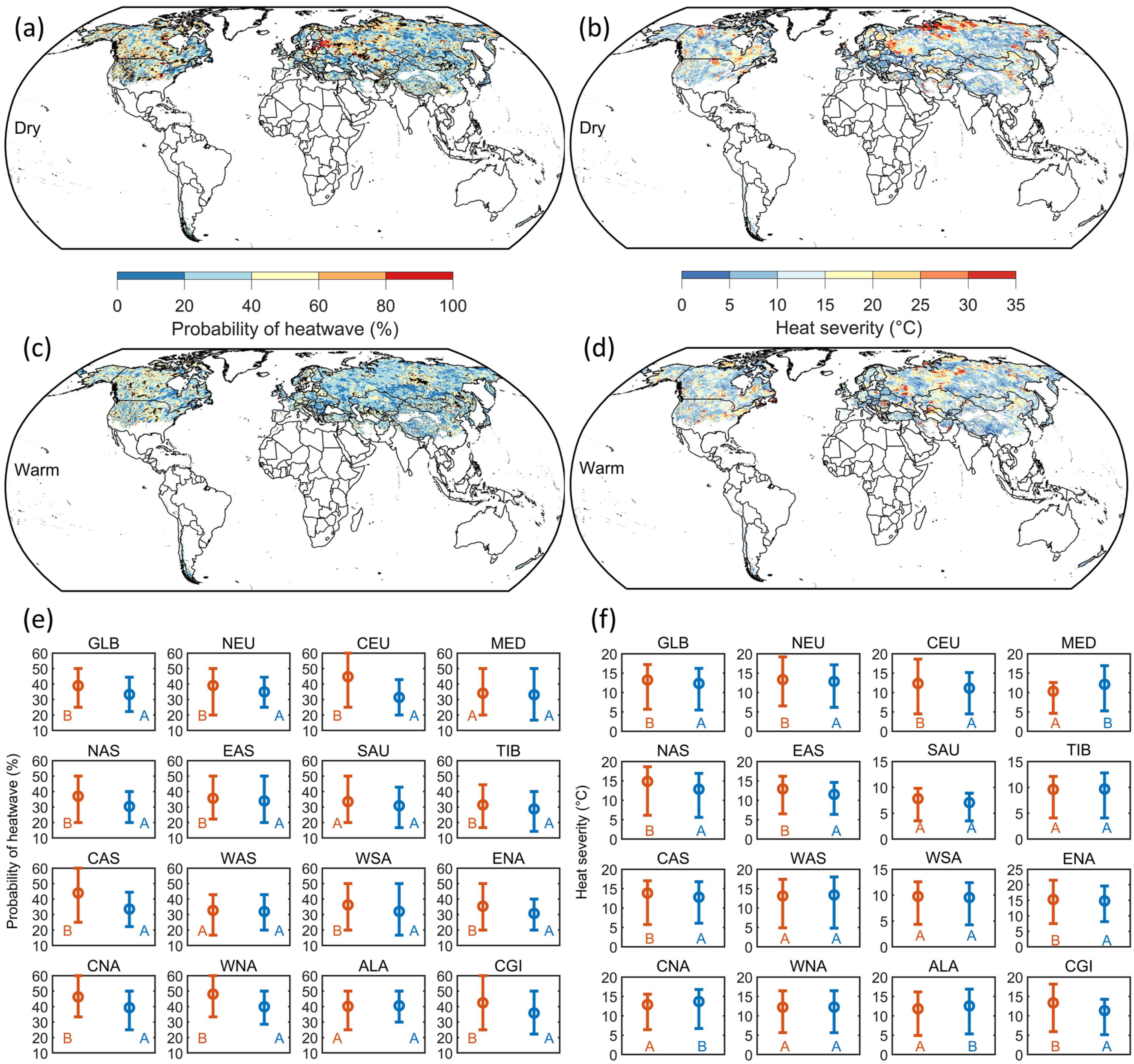

Figure 3. Heatwave probability (HWP, left column) and heatwave severity (HWS, right column) in dry- and warm-type compound snow drought and heatwave: HWP distribution under the type of dry (a) and warm (c) snow droughts; HWS distribution under the type of dry (b) and warm (d) snow droughts; HWP (e) and HWS (f) statistics under dry (red) and warm (blue) snow droughts. Statistically significant grid boxes at 95% confidence level are dotted on maps (a and c). The limits of statistics (e and f) represent the upper and lower quartiles and the circles represent the mean values. Statistics labeled with different letters ("A" and "B") indicate a significant difference, and letter "B" represents a greater mean value than letter "A." Two statistics that are both labeled with "A" have no obvious difference.

decreases (increases) and the SM (VPD) are significantly lower (higher) than those of all grid boxes (Figures 4a and 4c). The warm snow drought has less and sometimes adverse effects on soil drought and atmospheric aridity (Figures 4b and 4d), which may result from the offset by near-normal or above-normal precipitation. Such effects of dry and warm snow droughts on SM and VPD can be seen in all sub-regions, especially in Asia and North America (Figures S8 and S9 in Supporting Information S1).

We further examined the correlations between HWS and SM/VPD anomalies (Figures 4e and 4f, S10, and S11 in Supporting Information S1). Heatwave severity has a significant positive correlation with VPD anomaly and a significant negative correlation with SM anomaly globally. And the correlations become stronger under dry

10.1029/2022GL099925

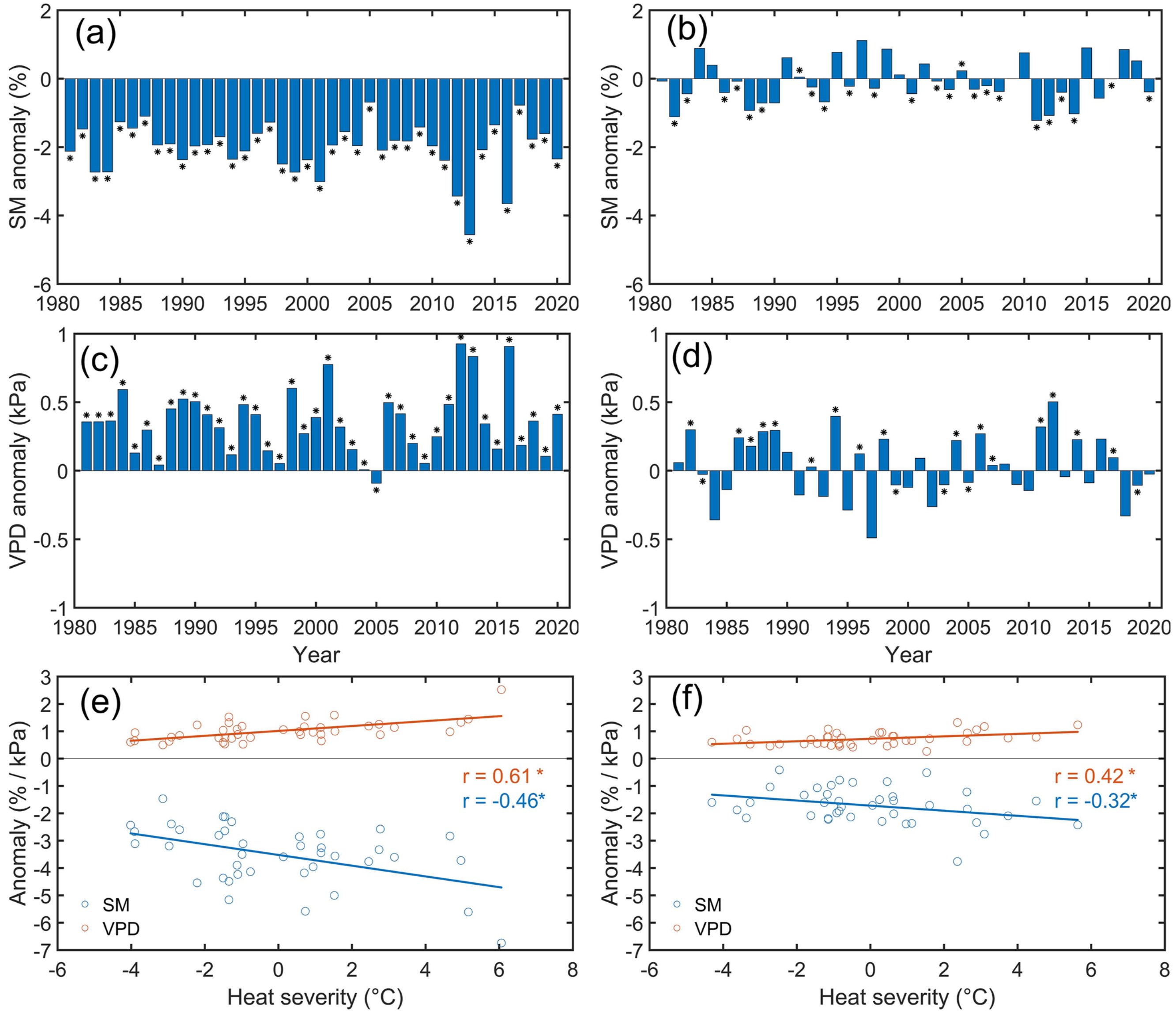

Figure 4. Soil moisture (SM) anomaly (a and b) and vapor pressure deficit (VPD) anomaly (c and d) as well as their correlations with heatwave severity (e and f) in the first snow-free month under dry (left column) and warm (right column) snow drought conditions. Asterisks in a–d denote that the SM (VPD) of snow-drought grid boxes is significant ($p < 0.05$) lower (higher) than those of all grid boxes based on the two-sample *t*-test. Asterisks in e and f represent that the correlation is statistically significant ($p < 0.05$). Linear trends have been removed from all the variables.

snow drought conditions than those under warm snow drought conditions (Figures 4e and 4f). The correlation varies regionally across the globe (Figures S10 and S11 in Supporting Information S1). The regions of Asia (e.g., NAS, EAS, TIB, and CAS) usually have a significant correlation with both VPD and SM anomalies. The regions of North America including ENA, CNA, ALA and CGI, however, only show a significant correlation with VPD anomaly. Our findings indicate a possible mechanism that snow drought could exacerbate soil drought and atmospheric aridity and thus promote the successive heatwave, especially when dry snow drought occurs.

4. Discussion and Concluding Remarks

Snow drought and heatwave have been receiving increasing attention in recent years, but they are usually treated individually. This study provides a comprehensive assessment of CSDHW (snow drought followed by heatwave) events on a global scale. Through coincidence detection and attribution analysis in 15 reference regions and eight regional hotspots (Text S2 in Supporting Information S1), we show the probability of occurrence, spatiotemporal changes, and possible mechanisms of CSDHW for the period of 1981–2020. We find an average of 35% of all snow droughts followed by heatwaves. An expansion of the coverage of CSDHW is detected globally, with a significant increase in Eurasia and a relatively high fluctuation in North America. Furthermore, the warm-type CSDHW occurs more frequently than the dry-type CSDHW, with a greater increasing trend in coverage fraction. Our findings reveal that dry snow drought is more likely to be followed by heatwave because it tends to promote the successive heatwave associated with the intensified soil drought and atmospheric aridity.

In this study, we used the state-of-the-art ERA5-Land data set, which is featured with flexible spatial and temporal resolution (Muñoz-Sabater et al., 2021) and good performance in identifying extreme temperature events (Sheridan et al., 2020). More importantly, the SWE of ERA5-Land agrees better with station observations compared with other datasets (Shao et al., 2022), making it an ideal data set to characterize snow droughts. To further demonstrate the robustness of our results, we compared the CSDHW events detected based on ERA5-Land with those by chance (You & Wang, 2021). We randomly resampled the time series of snow droughts and heatwaves 1,000 times. The mean probability of occurrence of CSDHW events of the 1,000 realizations was calculated and then compared with the detected results. We find that the detected probability of CSDHW events is significantly different ($p < 0.05$) from those of random coincidences (58% detected vs. 32% random mean, see Figure S12 in Supporting Information S1), indicating that the detected CSDHW events are not pure coincidence.

We show that late winter snow drought contributes to soil drought and atmospheric aridity in early spring (Figures 4a–4d), which plays an important role in the occurrence of the following heatwave after snow drought (Figures 4e and 4f). Abnormally low snowpack during a snow drought is expected to decrease the albedo and increase the net solar radiation of land surface, which directly contributes to elevating air temperature (Dutra et al., 2011; Xu & Dirmeyer, 2011) and thus increasing the frequency of extreme hot events (Diffenbaugh et al., 2005). Lower SM induced by less snowmelt would be conducive to warming the atmosphere by reduced evaporative cooling and increased sensible heating of the surface (Teuling, 2018), which could potentially promote heatwave occurrence (Santanello et al., 2018; Seneviratne et al., 2010) and even prolong the extreme heat because of SM memory (Lorenz et al., 2010). This causal link between SM and heatwaves has been widely identified by observational and simulation studies (Dirmeyer et al., 2021; Hirsch et al., 2019; Stegehuis et al., 2021; Wehrli et al., 2019). Comparatively high temperature along with atmospheric moisture deficit of dry snow drought increases the evaporative demand of atmosphere (represented by VPD in this study), which in turn amplifies the warming (Chiang et al., 2018; Mukherjee & Mishra, 2021) and favors hot days by depleting SM and closing plant stomata (Lansu et al., 2020; Stegehuis et al., 2021). It should be noted that large-scale atmospheric circulations, such as blocking highs, atmospheric stagnation, planetary wave, and subtropical highs, are also responsible for the occurrence of land-based heatwaves (Zhang et al., 2021). These anomalies of atmospheric circulation could result from the internal variability of atmospheric circulation as well as the ocean conditions via teleconnections (Wehrli et al., 2019). Besides, snow drought does not necessarily lead to significant changes in SM and VPD of the first snow-free month in some regions and years (Figures S8 and S9 in Supporting Information S1). Antecedent land surface and atmospheric conditions (e.g., SM and VPD of the last snow-covered month) also play an important role in exacerbating the subsequent heatwaves by increasing the likelihood and persistence of exceptionally high temperatures (Fischer et al., 2007; Hauser et al., 2016; Hirsch et al., 2019; Lorenz et al., 2010). Our attribution analysis associated with soil drought and atmospheric aridity provide insights into the underlying mechanisms from a general perspective of land–atmosphere feedbacks on a global scale.

This study indicates a more frequent sequential occurrence of snow drought and heatwave under a warming climate. Our findings provide scientific evidence and guideline for adaptation to the multiplying risk of the sequential occurrence of snow drought and heatwave. The possible mechanisms provide implications for better understanding and forewarning the emerging compound hazard. Nevertheless, more attribution analyses are needed to further improve the process understanding and risk mitigation of CSDHW events in the future.

Data Availability Statement

Data in this study are accessible at: (a) ERA5-Land: https://cds.climate.copernicus.eu/cdsapp#!/dataset/reanalysis-era5-land-monthly-means?tab=overview; (b) the MODIS Snow Cover: https://nsidc.org/data/MOD10CM/versions/6; (c) Reference regions of IPCC AR5: https://www.ipcc-data.org/guidelines/pages/ar5_regions.html;

(d) Climatic Research Unit Time-Series version 4.05 (CRU TS4.05): https://catalogue.ceda.ac.uk/uuid/c26a65020a5e4b80b20018f148556681.

Acknowledgments

This research was supported by the National Natural Science Foundation of China (Grant No. 51809223) and the Hong Kong Research Grants Council Early Career Scheme (Grant No. 25222319).

References

Barnett, T. P., Adam, J. C., & Lettenmaier, D. P. (2005). Potential impacts of a warming climate on water availability in snow-dominated regions. *Nature*, *438*(7066), 303–309. https://doi.org/10.1038/nature04141

Chen, Y., & Zhai, P. (2017). Revisiting summertime hot extremes in China during 1961–2015: Overlooked compound extremes and significant changes. *Geophysical Research Letters*, *44*(10), 5096–5103. https://doi.org/10.1002/2016GL072281

Chiang, F., Mazdiyasni, O., & AghaKouchak, A. (2018). Amplified warming of droughts in southern United States in observations and model simulations. *Science Advances*, *4*(8), eaat2380. https://doi.org/10.1126/sciadv.aat2380

Christensen, J. H., Kumar, K. K., Aldrian, E., An, S.-I., Cavalcanti, I. F. A., Castro, M. d., et al. (2013). Climate phenomena and their relevance for future regional climate change. In T. F. Stocker, D. Qin, G.-K. Plattner, M. Tignor, S. K. Allen, J. Boschung, et al. (Eds.), *Climate change 2013: The physical science basis. Contribution of working group I to the fifth assessment report of the intergovernmental panel on climate change*. Cambridge University Press.

Déry, S. J., & Brown, R. D. (2007). Recent Northern Hemisphere snow cover extent trends and implications for the snow-albedo feedback. *Geophysical Research Letters*, *34*(22), L22504. https://doi.org/10.1029/2007GL031474

Dierauer, J. R., Allen, D. M., & Whitfield, P. H. (2019). Snow drought risk and susceptibility in the Western United States and Southwestern Canada. *Water Resources Research*, *55*(4), 3076–3091. https://doi.org/10.1029/2018WR023229

Diffenbaugh, N. S., Pal, J. S., Trapp, R. J., & Giorgi, F. (2005). Fine-scale processes regulate the response of extreme events to global climate change. *Proceedings of the National Academy of Sciences of the United States of America*, *102*(44), 15774–15778. https://doi.org/10.1073/pnas.0506042102

Dirmeyer, P. A., Balsamo, G., Blyth, E. M., Morrison, R., & Cooper, H. M. (2021). Land-atmosphere interactions exacerbated the drought and heatwave over Northern Europe during summer 2018. *AGU Advances*, *2*(2), e2020AV000283. https://doi.org/10.1029/2020AV000283

Donges, J. F., Schleussner, C.-F., Siegmund, J. F., & Donner, R. V. (2016). Event coincidence analysis for quantifying statistical interrelationships between event time series. *The European Physical Journal Special Topics*, *225*(3), 471–487. https://doi.org/10.1140/epjst/e2015-50233-y

Dutra, E., Schär, C., Viterbo, P., & Miranda, P. M. A. (2011). Land-atmosphere coupling associated with snow cover. *Geophysical Research Letters*, *38*(15), L15707. https://doi.org/10.1029/2011GL048435

Fischer, E. M., Seneviratne, S. I., Vidale, P. L., Lüthi, D., & Schär, C. (2007). Soil moisture–atmosphere interactions during the 2003 European summer heat wave. *Journal of Climate*, *20*(20), 5081–5099. https://doi.org/10.1175/JCLI4288.1

Francis, J. A., & Vavrus, S. J. (2012). Evidence linking Arctic amplification to extreme weather in mid-latitudes. *Geophysical Research Letters*, *39*(6), L06801. https://doi.org/10.1029/2012GL051000

Gleason, K. E., McConnell, J. R., Arienzo, M. M., Chellman, N., & Calvin, W. M. (2019). Four-fold increase in solar forcing on snow in western U.S. burned forests since 1999. *Nature Communications*, *10*(1), 2026. https://doi.org/10.1038/s41467-019-09935-y

Hall, D. K., & Riggs, G. A. (2015). MODIS/Terra snow cover monthly L3 global 0.05Deg CMG, Version 6. In D. K. Hall & G. A. Riggs (Eds.), *NASA National snow and ice data center distributed active*. Archive Center.

Harpold, A., Dettinger, M., & Rajagopal, S. (2017). Defining snow drought and why it matters. *Eos Transactions American Geophysical Union*, *98*, 15–17. https://doi.org/10.1029/2017EO068775

Hauser, M., Orth, R., & Seneviratne, S. I. (2016). Role of soil moisture versus recent climate change for the 2010 heat wave in western Russia. *Geophysical Research Letters*, *43*(6), 2819–2826. https://doi.org/10.1002/2016GL068036

He, X., & Sheffield, J. (2020). Lagged compound occurrence of droughts and pluvials globally over the past seven decades. *Geophysical Research Letters*, *47*(14), e2020GL087924. https://doi.org/10.1029/2020gl087924

Henderson, G. R., Peings, Y., Furtado, J. C., & Kushner, P. J. (2018). Snow–atmosphere coupling in the Northern Hemisphere. *Nature Climate Change*, *8*(11), 954–963. https://doi.org/10.1038/s41558-018-0295-6

Hirsch, A. L., Evans, J. P., Di Virgilio, G., Perkins-Kirkpatrick, S. E., Argüeso, D., Pitman, A. J., et al. (2019). Amplification of Australian heatwaves via local land-atmosphere coupling. *Journal of Geophysical Research: Atmospheres*, *124*, 13625–13647. https://doi.org/10.1029/2019JD030665

Horton, R. M., Mankin, J. S., Lesk, C., Coffel, E., & Raymond, C. (2016). A review of recent advances in research on extreme heat events. *Current Climate Change Reports*, *2*(4), 242–259. https://doi.org/10.1007/s40641-016-0042-x

Huning, L. S., & AghaKouchak, A. (2020). Global snow drought hot spots and characteristics. *Proceedings of the National Academy of Sciences*, *117*(33), 19753. https://doi.org/10.1073/pnas.1915921117

Jaeger, E. B., & Seneviratne, S. I. (2011). Impact of soil moisture–atmosphere coupling on European climate extremes and trends in a regional climate model. *Climate Dynamics*, *36*(9), 1919–1939. https://doi.org/10.1007/s00382-010-0780-8

Kovats, R. S., & Hajat, S. (2008). Heat stress and public health: A critical review. *Annual Review of Public Health*, *29*(1), 41–55. https://doi.org/10.1146/annurev.publhealth.29.020907.090843

Lansu, E. M., van Heerwaarden, C. C., Stegehuis, A. I., & Teuling, A. J. (2020). Atmospheric aridity and apparent soil moisture drought in European forest during heat waves. *Geophysical Research Letters*, *47*(6), e2020GL087091. https://doi.org/10.1029/2020GL087091

LeComte, D. (2011). Global Weather highlights 2010: Flooding, heatwaves, and fires. *Weatherwise*, *64*(3), 21–28. https://doi.org/10.1080/00431672.2011.566814

Lorenz, R., Jaeger, E. B., & Seneviratne, S. I. (2010). Persistence of heat waves and its link to soil moisture memory. *Geophysical Research Letters*, *37*(9), L09703. https://doi.org/10.1029/2010GL042764

Malek, K., Reed, P., Adam, J., Karimi, T., & Brady, M. (2020). Water rights shape crop yield and revenue volatility tradeoffs for adaptation in snow dependent systems. *Nature Communications*, *11*(1), 3473. https://doi.org/10.1038/s41467-020-17219-z

Marshall, A. M., Abatzoglou, J. T., Link, T. E., & Tennant, C. J. (2019). Projected changes in Interannual variability of peak snowpack amount and timing in the Western United States. *Geophysical Research Letters*, *46*(15), 8882–8892. https://doi.org/10.1029/2019GL083770

Matsumura, S., & Yamazaki, K. (2012). Eurasian subarctic summer climate in response to anomalous snow cover. *Journal of Climate*, *25*(4), 1305–1317. https://doi.org/10.1175/2011JCLI4116.1

Mote, P. W., Li, S., Lettenmaier, D. P., Xiao, M., & Engel, R. (2018). Dramatic declines in snowpack in the western US. *npj Climate and Atmospheric Science*, *1*(1), 2. https://doi.org/10.1038/s41612-018-0012-1

Mote, P. W., Rupp, D. E., Li, S., Sharp, D. J., Otto, F., Uhe, P. F., et al. (2016). Perspectives on the causes of exceptionally low 2015 snowpack in the western United States. *Geophysical Research Letters*, *43*(20), 10980–10988. https://doi.org/10.1002/2016GL069965

Mukherjee, S., & Mishra, A. K. (2021). Increase in compound drought and heatwaves in a warming world. *Geophysical Research Letters*, *48*(1), e2020GL090617. https://doi.org/10.1029/2020GL090617

Muñoz-Sabater, J., Dutra, E., Agustí-Panareda, A., Albergel, C., Arduini, G., Balsamo, G., et al. (2021). ERA5-Land: A state-of-the-art global reanalysis dataset for land applications. *Earth System Science Data*, *13*(9), 4349–4383. https://doi.org/10.5194/essd-13-4349-2021

Nexus Media. (2018). California's dwindling snowpack: Another year of drought, floods, wildfires and mudslides? Retrieved from https://www.ecowatch.com/california-weather-snow-climate-change-2558329229.html

Oakley, N. S., Lancaster, J. T., Kaplan, M. L., & Ralph, F. M. (2017). Synoptic conditions associated with cool season post-fire debris flows in the Transverse Ranges of southern California. *Natural Hazards*, *88*(1), 327–354. https://doi.org/10.1007/s11069-017-2867-6

Perkins-Kirkpatrick, S. E., & Lewis, S. C. (2020). Increasing trends in regional heatwaves. *Nature Communications*, *11*(1), 3357. https://doi.org/10.1038/s41467-020-16970-7

Qi, W., Feng, L., Liu, J., & Yang, H. (2020). Snow as an important natural reservoir for runoff and soil moisture in Northeast China. *Journal of Geophysical Research: Atmospheres*, *125*, e2020JD033086. https://doi.org/10.1029/2020JD033086

Raymond, C., Horton, R. M., Zscheischler, J., Martius, O., AghaKouchak, A., Balch, J., et al. (2020). Understanding and managing connected extreme events. *Nature Climate Change*, *10*(7), 611–621. https://doi.org/10.1038/s41558-020-0790-4

Robinson, P. J. (2001). On the definition of a heat wave. *Journal of Applied Meteorology*, *40*(4), 762–775. https://doi.org/10.1175/1520-0450(2001)040<0762:OTDOAH>2.0.CO;2

Santanello, J. A., Dirmeyer, P. A., Ferguson, C. R., Findell, K. L., Tawfik, A. B., Berg, A., et al. (2018). Land–atmosphere interactions: The LoCo perspective. *Bulletin of the American Meteorological Society*, *99*(6), 1253–1272. https://doi.org/10.1175/BAMS-D-17-0001.1

Seneviratne, S. I., Corti, T., Davin, E. L., Hirschi, M., Jaeger, E. B., Lehner, I., et al. (2010). Investigating soil moisture–climate interactions in a changing climate: A review. *Earth-Science Reviews*, *99*(3), 125–161. https://doi.org/10.1016/j.earscirev.2010.02.004

Shao, D., Li, H., Wang, J., Hao, X., Che, T., & Ji, W. (2022). Reconstruction of a daily gridded snow water equivalent product for the land region above 45°N based on a ridge regression machine learning approach. *Earth System Science Data*, *14*(2), 795–809. https://doi.org/10.5194/essd-14-795-2022

Sheridan, S. C., Lee, C. C., & Smith, E. T. (2020). A comparison between station observations and reanalysis data in the identification of extreme temperature events. *Geophysical Research Letters*, *47*(15), e2020GL088120. https://doi.org/10.1029/2020GL088120

Siegmund, J. F., Siegmund, N., & Donner, R. V. (2017). CoinCalc—A new R package for quantifying simultaneities of event series. *Computers & Geosciences*, *98*, 64–72. https://doi.org/10.1016/j.cageo.2016.10.004

Smith, T., Bookhagen, B., & Rheinwalt, A. (2017). Spatiotemporal patterns of High Mountain Asia's snowmelt season identified with an automated snowmelt detection algorithm, 1987–2016. *The Cryosphere*, *11*(5), 2329–2343. https://doi.org/10.5194/tc-11-2329-2017

Stegehuis, A. I., Vogel, M. M., Vautard, R., Ciais, P., Teuling, A. J., & Seneviratne, S. I. (2021). Early summer soil moisture contribution to western European summer warming. *Journal of Geophysical Research: Atmospheres*, *126*, e2021JD034646. https://doi.org/10.1029/2021JD034646

Tang, Q., Zhang, X., & Francis, J. A. (2014). Extreme summer weather in northern mid-latitudes linked to a vanishing cryosphere. *Nature Climate Change*, *4*(1), 45–50. https://doi.org/10.1038/nclimate2065

Teuling, A. J. (2018). A hot future for European droughts. *Nature Climate Change*, *8*(5), 364–365. https://doi.org/10.1038/s41558-018-0154-5

The Guardian. (2022). Record temperatures forecast as winter heatwave heads for California Retrieved from https://www.theguardian.com/us-news/2022/feb/09/california-winter-heatwave-record-temperatures-forecast

Toure, A. M., Reichle, R. H., Forman, B. A., Getirana, A., & De Lannoy, G. J. M. (2018). Assimilation of MODIS snow cover fraction observations into the NASA catchment land surface model. *Remote Sensing*, *10*(2), 316. https://doi.org/10.3390/rs10020316

Trujillo, E., Molotch, N. P., Goulden, M. L., Kelly, A. E., & Bales, R. C. (2012). Elevation-dependent influence of snow accumulation on forest greening. *Nature Geoscience*, *5*(10), 705–709. https://doi.org/10.1038/ngeo1571

Wehrli, K., Guillod, B. P., Hauser, M., Leclair, M., & Seneviratne, S. I. (2019). Identifying key driving processes of major recent heat waves. *Journal of Geophysical Research: Atmospheres*, *124*, 11746–11765. https://doi.org/10.1029/2019JD030635

Wlostowski, A. N., Jennings, K. S., Bash, R. E., Burkhardt, J., Wobus, C. W., & Aggett, G. (2022). Dry landscapes and parched economies: A review of how drought impacts nonagricultural socioeconomic sectors in the US Intermountain West. *Wiley Interdisciplinary Reviews: Water*, *9*(1), e1571. https://doi.org/10.1002/wat2.1571

Xu, L., & Dirmeyer, P. (2011). Snow-atmosphere coupling strength in a global atmospheric model. *Geophysical Research Letters*, *38*(13), L13401. https://doi.org/10.1029/2011GL048049

You, J., & Wang, S. (2021). Higher probability of occurrence of hotter and shorter heat waves followed by heavy rainfall. *Geophysical Research Letters*, *48*(17), e2021GL094831. https://doi.org/10.1029/2021GL094831

Yuan, W., Zheng, Y., Piao, S., Ciais, P., Lombardozzi, D., Wang, Y., et al. (2019). Increased atmospheric vapor pressure deficit reduces global vegetation growth. *Science Advances*, *5*(8), eaax1396. https://doi.org/10.1126/sciadv.aax1396

Zhang, R., Sun, C., Zhu, J., Zhang, R., & Li, W. (2020). Increased European heat waves in recent decades in response to shrinking Arctic sea ice and Eurasian snow cover. *NPJ Climate and Atmospheric Science*, *3*(1), 7. https://doi.org/10.1038/s41612-020-0110-8

Zhang, W., Luo, M., Gao, S., Chen, W., Hari, V., & Khouakhi, A. (2021). Compound hydrometeorological extremes: Drivers, mechanisms and methods. *Frontiers of Earth Science*, *9*. https://doi.org/10.3389/feart.2021.673495

References From the Supporting Information

Qing, Y., Wang, S., Ancell, B., & Yang, Z.-L. (2022). Accelerating flash droughts induced by the joint influence of soil moisture depletion and atmospheric aridity. *Nature Communications*, *13*, 1139. https://doi.org/10.1038/s41467-022-28752-4

Svoboda, M., LeComte, D., Hayes, M., Heim, R., Gleason, K., Angel, J., et al. (2002). The drought monitor. *Bulletin of the American Meteorological Society*, *83*(8), 1181–1190. https://doi.org/10.1175/1520-0477-83.8.1181